

Rapid Collapse of a Plasma Sawtooth Oscillation in the JET Tokamak

A. W. Edwards, D. J. Campbell, W. W. Engelhardt, H.-U. Fahrbach,^(a) R. D. Gill, R. S. Granetz,^(b)
S. Tsuji,^(c) B. J. D. Tubbing,^(d) A. Weller,^(a) J. Wesson, and D. Zasche^(a)

JET Joint Undertaking, Abingdon, Oxon OX14 3EA, United Kingdom

(Received 28 March 1986)

The rapid collapse of a sawtooth oscillation in the JET tokamak has been observed in detail on a fast time scale. Tomographic reconstruction of data from two x-ray cameras and electron-cyclotron-emission temperature profiles show that during the sawtooth collapse the central hot region is rapidly (in approximately 100 μ s) displaced off axis with an $m = 1$ component and is then redistributed around a surface of constant minor radius. The theoretical implications of the measurements are discussed.

PACS numbers: 52.55.Fa, 52.30.Gz, 52.35.-g, 52.70.La

The sawtooth oscillation was first reported¹ on the ST tokamak and the basic features of a slowly rising central electron temperature followed by a rapid drop in temperature have been subsequently observed on many other tokamaks. The fast collapse was found to be described by an $m = n = 0$ mode. Kadomtsev² and others proposed a generally accepted theoretical model in which the rapid drop in central temperature was

seen as a consequence of a slowly growing $m = 1$ instability observed experimentally (see, e.g., Paré³) as a precursor oscillation to the sawtooth collapse. Recently, more complicated partial and giant or double sawteeth have been observed^{4,5} on the larger tokamaks. It has also been shown⁵ that the JET tokamak sawtooth collapse can occur without precursors and on a faster time scale than that expected from Kadomtsev's model. However, the detailed behavior of the plasma during the rapid collapse has remained obscure and in this Letter we report results of time-resolved tomographic x-ray reconstructions of the plasma emission and electron-cyclotron-emission (ECE) temperature-profile measurements, taken during the sawtooth collapse. The measurements provide important new information about the collapse mechanism and clearly show that the initial part of the collapse has an $m = 1$ mode which grows rapidly (in 100 μ s) followed by an equally rapid transition to a configuration with poloidal symmetry. These results have fundamentally new implications for the theoretical understanding of the sawtooth mechanisms.

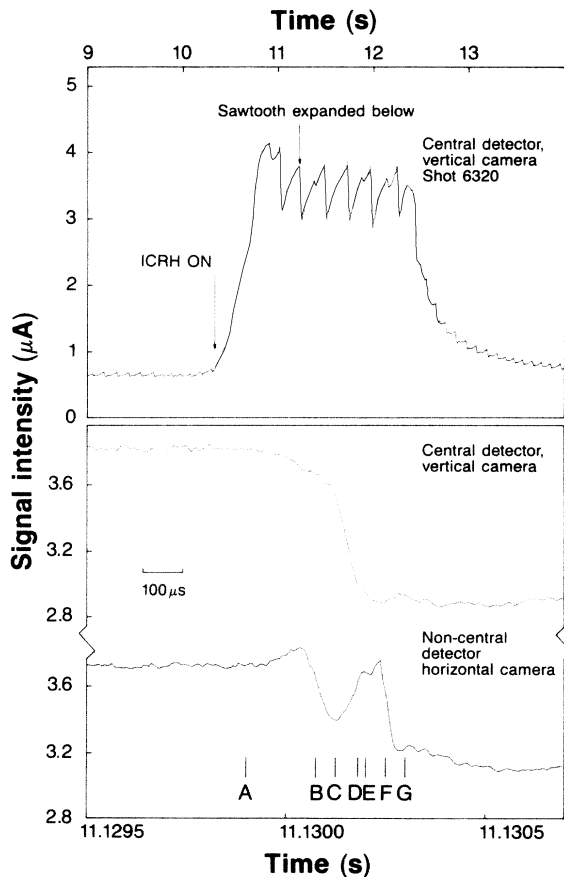


FIG. 1. X-ray signal intensity as a function of time. The lower two traces have the same very expanded time scale. The letters *A* to *G* indicate the reconstruction times for Figs. 3 and 4.

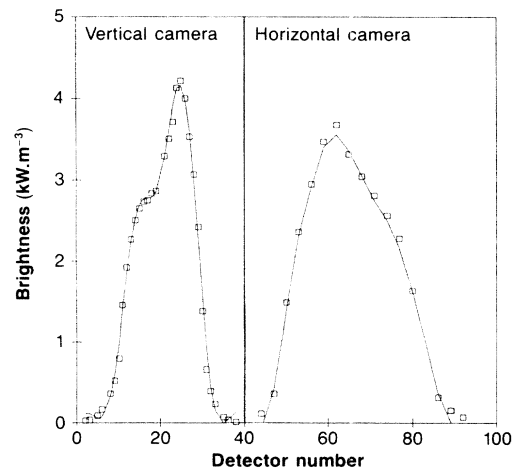


FIG. 2. X-ray brightnesses plotted vs detector number at $t = 11.130225$ s. The full line is the fit determined by the tomographic reconstruction.

TABLE I. Time scales and radiated power as a function of height and major radius. See Figs. 3 and 4 for profile identification.

Profile	Relative time (μs)	P_{max} ($\text{mW} \cdot \text{cm}^{-3}$)
A ^a	0	3.7
B	175	3.9
C	225	3.9
D	275	4.1
E	300	4.1
F	350	3.3
G	400	2.7
H	2980	2.1

^aProfile A is taken at $t = 11.1299$ s.

Measurement systems.—Two soft x-ray cameras⁶ view the plasma through Be filters from vertical and horizontal ports with a total of 100 silicon-diode detectors. The vertical camera contains 38 detectors and the horizontal camera 62. The spatial resolution is 7 cm. The detectors are calibrated to 0.5% and, after analog filtering with a bandwidth of less than 100 kHz, the signals are digitized at frequencies up to 200 kHz.

In addition, the plasma electron temperature, T_e , in the central region is measured (with 10% absolute and 5% relative error) by a twelve-channel ECE grating polychromator along a single midplane chord with a time resolution of 10 μs and spatial resolution of 8 cm.⁷

Tomographic analysis.—The signal observed in each

x-ray detector is a line integral of the emission transmitted through a 140- μm Be filter which has an energy threshold of 2.8 keV. For rf-heated discharges the observed intensity is mainly due to emission from He-like nickel. The x-ray measurements were carried out during a JET discharge with ion-cyclotron heating with parameters $R = 2.93$ m, $a = 1.23$ m, $b/a = 1.42$, $\bar{n}_e = 1.6 \times 10^{19} \text{ m}^{-3}$, $B = 2.9$ T, $I = 3.4$ MA, and $P_{\text{rf}} = 5.0$ MW.

The structure of the central region is studied with a tomographic method,⁸ which allows reconstruction of the x-ray emission without having to make assumptions about the symmetry or rotation of the plasma. The x-ray emission is described by Zernicke polynomials of order ml which determine the minor radial dependence and angular harmonics $\sin m\theta$ and $\cos m\theta$. The detector configuration on JET allows for reconstructions with $l = 8$ and the angular harmonics $m = 0, \cos\theta, \sin\theta, \cos 2\theta$. The inclusion of higher angular harmonics could lead to the generation of spurious features in the reconstructions. Data from 35 equispaced diodes in the vertical camera and nineteen in the horizontal camera are used.

The signal from a central x-ray detector (Fig. 1) of the vertical camera shows large-amplitude sawtooth oscillations without precursors. The expanded trace from the central detector shows the very rapid collapse occurring in $\sim 100 \mu\text{s}$, with no evidence of any plasma perturbation earlier than 100 μs before the start of the collapse. The trace from the noncentral channel shows much more complicated behavior as a result of the complex motion of the central region of the plas-

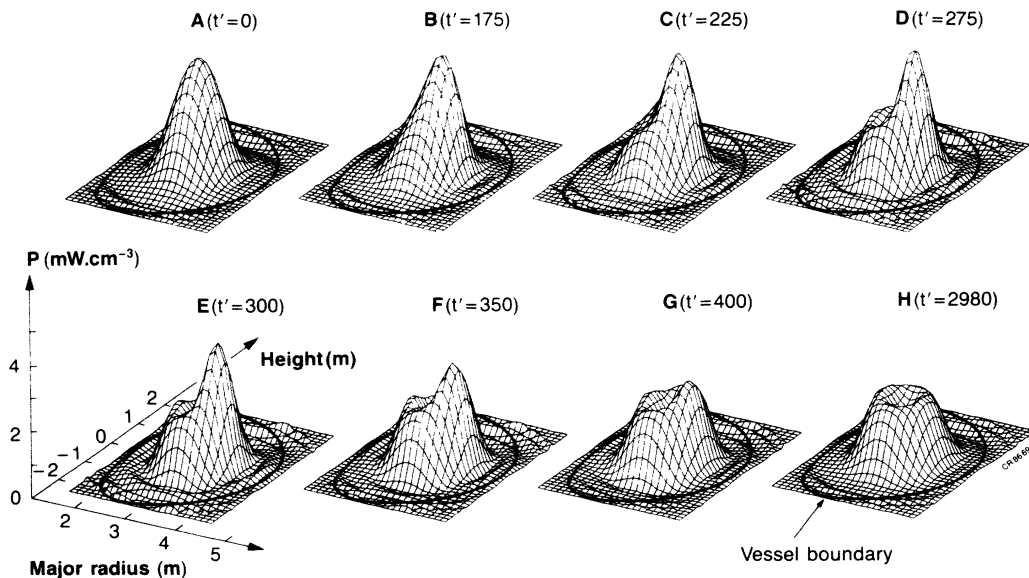


FIG. 3. Tomographically reconstructed 2D x-ray emission profiles. The first three frames (A–C) show the initial movement of the hot plasma center; the last five (D–H) show the collapse to a final poloidally symmetric state. Profile A is at $t = 11.129900$ s.

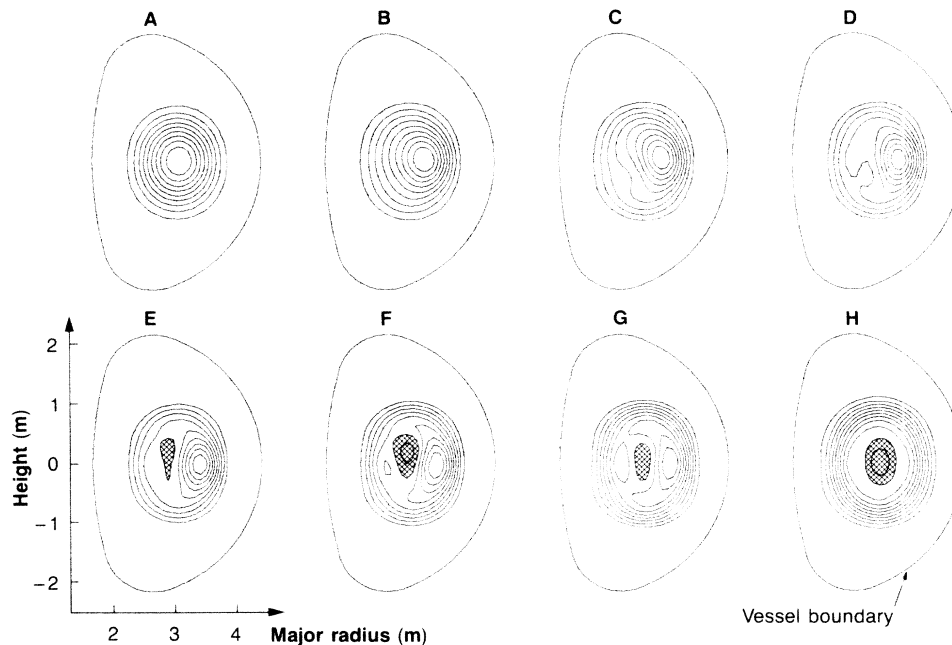


FIG. 4. Contour plots (with 10% contour intervals) of the tomographically reconstructed x-ray emission showing the initial plasma motion and the collapse to the final symmetric state (crosshatching indicates hollow profiles).

ma. In Fig. 2 the detector brightnesses are shown for both cameras during the sawtooth collapse together with the best fit to the data determined by the tomographic analysis. The plots of reconstructed x-ray emission made at the times shown in Table I and showing the radiated power, P , as a function of height and major radius (Figs. 3 and 4) clearly determine the topology of the sawtooth collapse and show that it occurs in essentially two phases. Initially the region of maximum emission, or hot spot, moves rapidly outward in minor radius until it reaches $r/a \approx 0.3$. A maximum velocity of up to $2.6 \times 10^3 \text{ m} \cdot \text{s}^{-1}$ is reached (Figs. 3 and 4, profiles A, B, and C). The volume of the moving hot spot and the maximum level of emission remain approximately constant. This phase has a very clear $m=1$ character. ECE measurements made at separate toroidal locations show that the collapse has $n=1$. For other sawteeth the initial plasma motion occurs with a variety of poloidal angles as expected for this mode.

In the second phase of the collapse (profiles D to H), the emission from the hot spot rapidly decreases with a time constant of $100 \mu\text{s}$, while the emission in the rest of the central region increases leaving a final poloidally symmetric profile H. Because the x-ray emission occurs from the hottest, densest parts of the plasma, these observations imply either rapid mixing of hot and cooler plasma or rapid conduction of heat from the hot regions. The final hollow profile of x-ray emission then becomes gradually more peaked as the plasma is heated until the next sawtooth collapse oc-

curs after 150 ms. Viewed overall, the effect of the sawtooth collapse is to change the initial peaked profile A with $P(\text{max}) = 3.7 \text{ mW} \cdot \text{cm}^{-3}$ to a final hollow profile H with $P(\text{max}) = 2.2 \text{ mW} \cdot \text{cm}^{-3}$.

Electron-temperature measurements in similar discharges also show the two phases of the collapse. A contour plot of T_e as a function of major radius and time (Fig. 5) shows a rapid inward movement of the plasma center followed by a rapid temperature collapse from $T_e = 4.3 \text{ keV}$ to $T_e = 3.0 \text{ keV}$. This is consistent with an $m=1$ mode and shows that the change in x-ray emission is mainly caused by a change in temperature. Other sawtooth collapses in discharges both with and without ion-cyclotron resonance heating (ICRH) show very similar behavior independent of the presence or absence of any precursor oscillations.

Our observations can be compared with different theoretical models. In the Kadomtsev model,² the magnetic flux inside and outside the $q=1$ surface is reconnected in a narrow layer with a thickness which in JET would be much less than 1% of the plasma radius. This layer is formed on the part of the $q=1$ surface towards which the central plasma is displaced. On the opposite side the reconnected flux forms a magnetic island which grows outward from the $q=1$ surface. The experimental observations are not consistent with this description. The time scale of the sawtooth collapse in the Kadomtsev model is somewhat uncertain but for the present case is the order of a few milliseconds which is very much longer than the observed collapse time of $100 \mu\text{s}$.

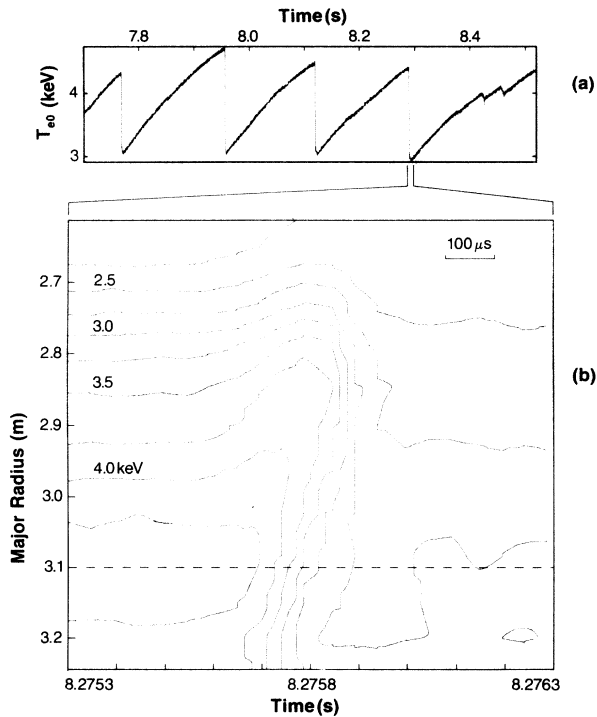


FIG. 5. (a) Central electron temperature. (b) Contour plot of T_e (ECE) vs major radius and time. The inward motion of the plasma and fast temperature collapse can be clearly seen.

In some models the collapse takes place with an already existing magnetic island.^{9,10} The emission profiles shown above give no indication of such a pre-existing perturbation. Another model¹¹ assumes that an $m = 1$ tearing mode grows until the associated island covers the central region. The precursor oscillations often observed in other tokamaks might then be attributed to the early phase of this growth. Our observations on sawteeth without precursors do not support this model.

The initial coherent displacement of the plasma on the observed short time scale suggests an ideal magnetohydrodynamic $m = 1$ instability. It was earlier believed that this mode would be stable but recent calculations¹² indicate that instability is possible provided q is close to unity across the central region. In this model a convective flow is triggered when q reaches unity and the hot core is replaced by a colder "bubble." This is quite similar to the behavior of the ob-

served x-ray emission but further investigations are required to confirm the details of this model.

It is a pleasure to acknowledge the considerable assistance we have received from our scientific and engineering colleagues at both IPP, Garching, and JET.

(a) Visitor from EURATOM-Institute für Plasmaphysik (IPP) Association, Garching, West Germany.

(b) Visitor from Massachusetts Institute of Technology, Cambridge, Massachusetts 02139.

(c) Visitor from Japan Atomic Energy Research Institute, Naka, Ibaraki, Japan.

(d) Visitor from EURATOM-Stichting voor Fundamenteel Onderzoek der Materie (FOM) Association, The Netherlands.

¹S. von Goeler, W. Stodiek, and N. Sauthoff, Phys. Rev. Lett. **33**, 1201 (1974).

²B. B. Kadomtsev, Fiz. Plazmy **1**, 710 (1975) [Sov. J. Plasma Phys. **1**, 389 (1975)].

³V. K. Paré, in *Magnetic Reconnection in Space and Laboratory Plasmas*, edited by E. W. Hones, Jr. (American Geophysical Union, Washington, 1984).

⁴W. Pfeiffer *et al.*, Nucl. Fusion **25**, 655 (1985); K. McGuire *et al.*, in Proceedings of the Twelfth European Conference on Controlled Fusion and Plasma Physics, Budapest, Hungary, 1985 (unpublished), Vol. 1, p. 134.

⁵D. J. Campbell *et al.*, in Proceedings of the Twelfth European Conference on Controlled Fusion and Plasma Physics, Budapest, Hungary, 1985 (unpublished), Vol. 1, p. 130; D. J. Campbell *et al.*, to be published.

⁶D. Zasche, H.-U. Fahrback, and E. Harmeyer, in Proceedings of the Thirteenth Symposium on Fusion Technology, Fusion Technol. **2**, 1103 (1984).

⁷B. J. D. Tubbing *et al.*, in Proceedings of the Twelfth European Conference on Controlled Fusion and Plasma Physics, Budapest, Hungary, 1985 (unpublished), Vol. 1, p. 215; A. E. Costley *et al.*, *ibid.*, p. 227.

⁸R. S. Granetz and J. F. Camacho, Nucl. Fusion **25**, 727 (1985).

⁹M. A. Dubois and A. Samain, Nucl. Fusion **20**, 1101 (1980).

¹⁰M. N. Bussac, R. Pellat, J. L. Soule, and M. Tagger, in *Magnetic Reconnection and Turbulence*, edited by Dubois *et al.* (Editions de Physique, Orsay, 1985).

¹¹B. V. Waddell, G. L. Jahns, J. D. Callen, and H. R. Hicks, Nucl. Fusion **18**, 735 (1978).

¹²J. A. Wesson, Plasma Phys. Controlled Fusion **28**, 243 (1986).